Heliyon 10 (2024) e30728

Contents lists available at ScienceDirect

Heliyon

journal homepage: www.cell.com/heliyon

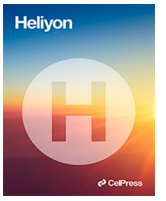

Research article

A modified orthotopic left lung transplantation model in rats

Jinsheng Li [1], Yifan Yu [1], Lingjun Dong, Zhiling Lou, Qiuyu Fang, Fuxiang Liang, Yangfan Li, Ming Wu [*]

Department of Thoracic Surgery, The Second Affiliated Hospital, Zhejiang University School of Medicine, Hangzhou, 310009, Zhejiang, China

ARTICLE INFO

Keywords:
Lung transplantation
Surgical technique
Model modification
Rat
Anastomosis

ABSTRACT

To enhance the operability of the rat orthotopic left lung transplantation model, we implemented several improvements and meticulously detailed the procedure. One hundred and thirty-one healthy male Sprague Dawley rats, weighing between 250 and 300 g, were utilized, with 64 serving as donors, 64 as recipients, and 3 as sham controls. We employed a modified three-cuff technique for the orthotopic left lung transplantation. Notably, our modified perfusion method could prevent donor lung edema, while waist-shaped cuffs minimized suture slippage during anastomosis. Additionally, positioning the recipient rat in a slightly left-elevated supine position during anastomosis reduced tension on the lung hilum, thus mitigating the risk of vascular laceration. The introduction of a unique two-person anastomosis technique significantly reduced operation time and substantially improved success rates. Furthermore, maximizing inflation of donor lungs both during preservation and surgery minimized the occurrence of postoperative atelectasis. Various other procedural refinements contributed to the enhanced operability of our model. Sixty-four rat orthotopic left lung transplantations were performed with only one surgical failure observed. The acquisition time for donor lungs averaged (19 ± 4) minutes, while (11 ± 1) minutes were allocated for donor lung hilum anatomy and cuff installation. Recipient thoracotomy and left lung hilar anatomy before anastomosis required (24 ± 8) minutes, with anastomosis itself taking (31 ± 6) minutes. Remarkably, the survival rate at the 4-h postoperative mark stood at 96.7 %. Even six months post-operation, transplanted left rat lungs continued to exhibit proper inflation and contraction rhythms, displaying signs of chronic pathological changes. In summary, our modified rat model of orthotopic left lung transplantation demonstrates robust operability, significantly reducing surgical duration, improving operation success rates, and enhancing postoperative survival rates. Furthermore, its long-term survival capacity enables the simulation of acute and chronic disease processes following lung transplantation.

1. Introduction

Lung transplantation stands as the foremost recourse for numerous end-stage lung ailments, encompassing advanced chronic obstructive pulmonary disease (COPD), idiopathic pulmonary fibrosis (IPF), and cystic pulmonary fibrosis (CPF) [1]. Despite a consistent annual rise in lung transplantations, the procedure still trails significantly behind other solid organ transplants like liver and kidney transplantation [2]. The primary challenges facing lung transplantation include a scarcity of donor lungs, donor lung injury,

* Corresponding author.
E-mail address: iwuming22@zju.edu.cn (M. Wu).
[1] J.L. and Y.Y. contributed equally.

https://doi.org/10.1016/j.heliyon.2024.e30728
Received 20 December 2023; Received in revised form 23 April 2024; Accepted 2 May 2024
Available online 9 May 2024

and the occurrence of primary graft dysfunction (PGD) [3]. Among the early acute complications post-transplantation, PGD emerges as the principal contributor to early postoperative mortality [4], while chronic lung allograft dysfunction (CLAD) stemming from chronic rejection poses a substantial threat to long-term patient survival [5].

Addressing the clinical dilemma of lung transplantation necessitates extensive basic research efforts. However, the domain of basic research on lung transplantation has not thrived. This stagnation can be largely attributed to the obstacles presented by animal models of lung transplantation. A cursory review of PubMed reveals approximately 100 papers utilizing rat or mouse kidney transplantation models in 2023, whereas only about 10 papers employ rat or mouse lung transplantation models within the same timeframe. Despite notable modifications in rodent lung transplantation models in recent years [6,7], there remains no discernible increase in the utilization of such models despite advancements in technology and economy. Conversely, there has been a significant rise in papers utilizing the lung hilar clamping model to simulate lung transplantation, owing to its simplicity [8]. However, it is crucial to acknowledge that the hilar clamping model fails to faithfully replicate the physiological intricacies of lung transplantation. This underscores the imperative for further refinement of rodent models of lung transplantation.

The rat orthotopic left lung transplantation model, which closely mimics the procedural and pathophysiological dynamics of human lung transplantation, represents a pivotal instrument for elucidating the mechanisms and therapies pertinent to lung injury post-transplantation. Nonetheless, the widespread adoption of this model is hindered by the intricate surgical maneuvers involved and the prolonged learning curve it entails [9]. To facilitate the broader utilization of the rat lung transplantation model, several challenges must be overcome:

The primary challenge is the steep learning curve associated with the utilization of surgical microscopes [10]. Surgeons often face interruptions during surgery to adjust the microscope, which prolongs the procedure [11]. Furthermore, the prohibitive cost of surgical microscopes renders them inaccessible to many researchers, discouraging them from attempting rat lung transplant techniques.

The second challenge arises from the unfamiliarity with the complex anatomical structure of the great cardiopulmonary vessels in rats. The intricate nature of these vessels poses difficulties for novices in distinguishing the structures that necessitate dissection. Although there are some studies offering diagrams of heart-lung vessels in rats [12], authentic anatomical photographs and videos of rat lung transplantation accompanied by detailed descriptions remain lacking.

Another obstacle is the absence of straightforward and effective anastomosis techniques [13]. While the transition from suturing [14] to employing cuffs [15] for anastomosis represents a revolutionary breakthrough in rat lung transplantation, the use of cuffs to anastomose also presents its own challenges. Although numerous researchers have endeavored to enhance anastomosis techniques, the complexity and intricacy of these methods may render them challenging to fully and accurately describe. Hence, there is an urgent need for a readily implementable and well-documented anastomosis technique, which could serve as a valuable reference for other rodent organ transplantation models, such as heart [16], liver [17], and kidney [18] transplantation.

Moreover, the rat left lung orthotopic transplantation model, despite its complexity, has often been inadequately described in previous methodological studies. Crucial details of the model, such as the method of endotracheal intubation, the cuffs' shape, and the technique for immobilizing the recipient left lung during anastomosis, have been overlooked. This omission necessitates subsequent researchers to conduct extensive massive exploratory experiments.

In our study, we address the aforementioned challenges encountered in orthotopic left lung transplantation in rats. We have refined nearly all facets of the model that may hinder researchers' understanding and meticulously described all key operational procedures. By doing so, we aim to encourage more researchers to grasp the intricacies of model preparation and apply it to their research endeavors.

2. Material and methods

2.1. Animals

We procured one hundred and thirty-one male Sprague Dawley (SD) rats, aged 8 weeks and weighing between 250 and 300 g, from the experimental animal center of Hangzhou Medical College (Hangzhou, China). These rats were housed in our specific pathogen-free (SPF) barrier facility, maintaining consistent environmental conditions (22–24 °C, relative humidity 45–55 %, with 12-h light/dark cycles). They had unrestricted access to water, and were provided with a meat-free rat and mouse diet (SF00-100, Specialty Feeds, Glen Forrest, Western Australia).

Sixty-four rats, with an average weight of (272 ± 11) g, were randomly assigned as donors, while 64 rats, with an average weight of (276 ± 12) g, were designated as recipients. We employed the modified three-cuff technique to execute orthotopic left lung transplantation. Operation-related time was meticulously recorded. Additionally, three rats underwent sham operations to serve as controls.

Among the 64 lung-transplanted rats, sixty-one were euthanized 4 h post-operation for sampling. Three rats underwent imagological examinations, while two were sacrificed for histopathological examination, one day and six months post-operation respectively.

2.2. Reagents and instruments

We prepared a low-potassium dextran (LPD) solution comprising Dextran-40 (50 g/L), Mannitol (20 mM), Glucose (5 mM), NaCl (136 mM), KCl (6 mM), $MgSO_4$ (800 μM), $Na_2HPO_4{\cdot}12H_2O$ (800 μM), $NaHCO_3$ (1 mM), and $CaCl_2$ (300 μM). The pH of the LPD solution was adjusted to 7.2–7.4. Subsequently, the LPD solution underwent filtration using a 0.22 μm filter membrane to eliminate

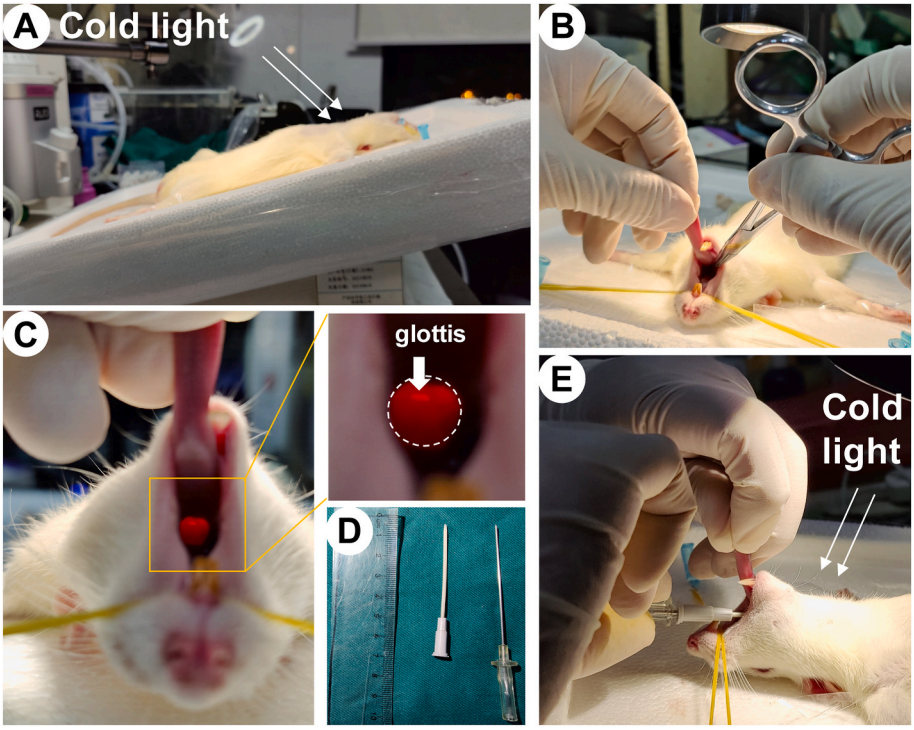

Fig. 1. Rat endotracheal intubation. A: During endotracheal intubation, the rat should be tilted at 30°, at a dorsal elevated position. The cold light is shone on the front of the neck. B: The rat's tongue was tightened. The glottis, a bright light spot, can be seen under the cold light. The glottis is indicated with a white arrow, the bright light spot is circled with a dashed line. C: The rat's throat was gently detached by an instrument. D: The endotracheal intubation tube was inserted directly when the larynx was open. E: Endotracheal intubation tube was made from the 16 G intravenous catheter with the tip of the needle worn down.

bacteria and was then stored at 4 °C. All the aforementioned substances were procured from Sinopharm Chemical Reagent Co., Ltd. (Shanghai, China).

We acquired pentobarbital sodium salt (P3761, Sigma-Aldrich), atropine sulfate monohydrate (u1045009, Sinopharm Chemical Reagent Co., Ltd.), and heparin sodium salt (63007131, Sinopharm Chemical Reagent Co., Ltd.). Disposable intravenous infusion needles (1.2 mm × 28 mm, TWSB) were sourced from Zhejiang Kindly Medical Devices Co., Ltd. (Wenzhou, China). Additionally, intravenous catheters (BD AngiocathTM, 14G, 16G; BD Intima-IITM, 18G) were purchased from Becton Dickinson MEDICAL DEVICES Co., Ltd. (Shanghai, China). The ventilator (R415 VentStar Small Animal Ventilator) and inhalation anesthesia device for small animals (R500 Small Animal Anesthesia Machine) were obtained from RWD Life Science Co., LTD. (Shenzhen, China). Microsurgical operation instruments and the blepharostat were procured from Ningbo Cheng-He Microsurgical Instruments Factory (Ningbo, China). Furthermore, micro hemostatic clips (W40080) were sourced from Shanghai Medical Instrument (Group) Co., Ltd. (Shanghai, China). We utilized Micro-CT (U-CT-XUHR, MILabs, Houten, The Netherlands) in this study.

2.3. Experimental setting

Under sterile conditions, a single surgeon, assisted by a colleague, conducted all operations. Time intervals were categorized as follows: 1) the duration for donor lung acquisition encompassed the period from incising the donor's abdominal vena cava and aortaventralis to submerging the donor's heart-lung block in the 4 °C LPD solution; 2) the timeframe for donor lung hilum anatomy and cuff installation extended from retrieving the heart-lung block from the preservation solution for hilar structure preparation to completing cuff placement; 3) the interval for recipient thoracotomy and left lung hilar anatomy comprised the duration from making a skin incision along the recipient's third rib interspace to incising the recipient's left pulmonary vein for anastomosis; 4) the time allocated for anastomosis commenced from incising the recipient's left pulmonary vein and positioning the donor's left lung adjacent to the incision, concluding with the restoration of perfusion.

2.4. Preoperative management and anesthesia

The rats underwent an 8-h fasting period. Thirty minutes before administering anesthesia, intraperitoneal administration of atropine sulfate monohydrate was performed at a dosage of 1 mg/kg. Anesthesia initiation entailed intraperitoneal injection of pentobarbital sodium at a dosage of 30 mg/kg.

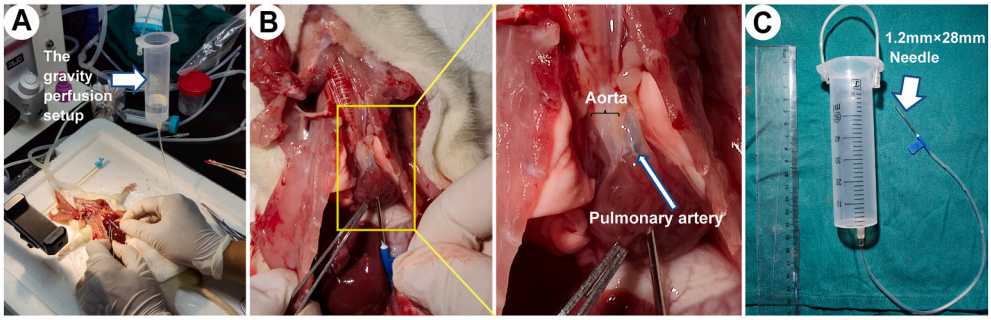

Fig. 2. Cold and heparinized LPD (Low-Potassium Dextran) solution was flushed into the pulmonary artery using the gravity perfusion setup. A and B: The left hand fixed the heart with forceps, and the right hand held the perfusion needle to puncture into the pulmonary artery to start perfusion. C: The gravity perfusion setup was made with a 50 mL syringe and a disposable intravenous infusion needle.

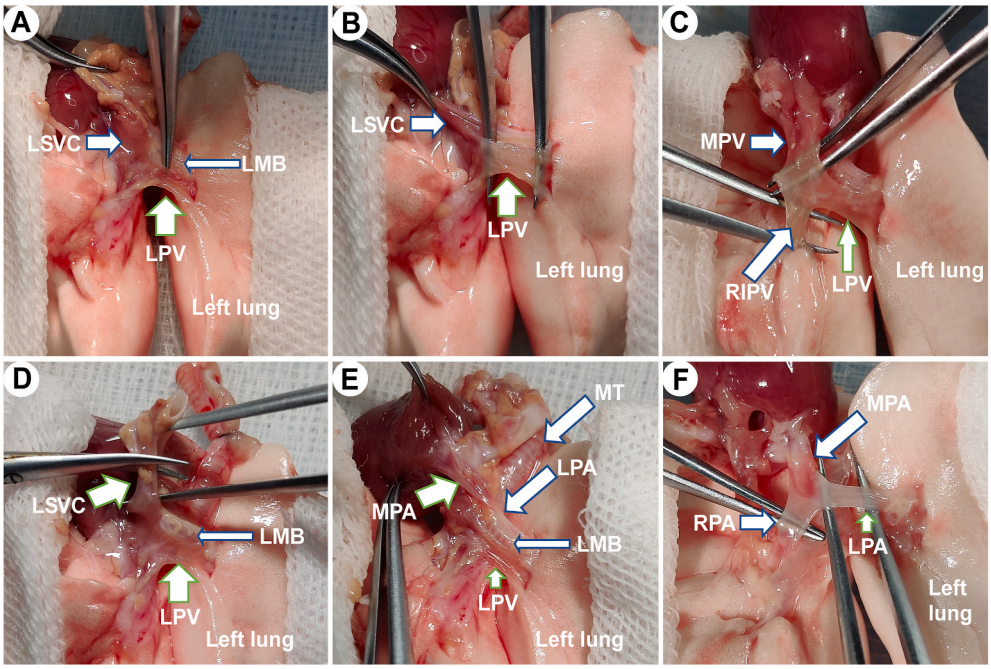

Fig. 3. Dissection of the left pulmonary vein and artery of the donor. A–B: The tips of the micro-forceps were inserted into the border between the left main bronchus (LMB) and the left pulmonary vein (LPV) to separate the left pulmonary vein. The left superior vena cava (LSVC) overlaid the main pulmonary vein (MPV). C: After stripping the left superior vena cava covering on the main pulmonary vein, the main pulmonary vein, which divides into the left pulmonary vein and the right inferior pulmonary vein (RIPV) at the end, was exposed. The pulmonary vein had only one branch on the left side. D and E: The left superior vena cava was cut off to expose the pulmonary artery. The main trachea (MT) was below the great vessels. F: After the pulmonary vein was stripped, the main pulmonary artery (MPA), which divides into the left pulmonary artery (LPA) and the right pulmonary artery (RPA), was exposed.

2.5. Endotracheal intubation and anesthesia maintaining

Following successful anesthesia induction, we secured the rat (either donor or recipient) onto the operating plate. The plate was inclined at a 30° angle, positioning the rat in a feet-down tilt orientation. Subsequently, we shaved the hair on the rat's anterior neck region and directed cold light vertically onto the area (Fig. 1A). Gently pulling out the rat's tongue, we immobilized it with the operator's left thumb and forefinger, lifting the pharynx with vascular forceps to expose the larynx (Fig. 1B). At this juncture, we observed the opening and closing of the larynx synchronized with the rat's breathing rhythm (Fig. 1C). As the larynx opened, we inserted the endotracheal intubation tube (Fig. 1D) directly into it under direct visualization (Fig. 1E). Finally, we secured the endotracheal intubation tube in place and configured the ventilator parameters as follows: tidal volume of 10 mL/kg of air, respiratory rate of 90 breaths/minute, positive end-expiratory pressure (PEEP) of 3 cm H_2O, and maintenance of anesthesia with 2 % isoflurane gas.

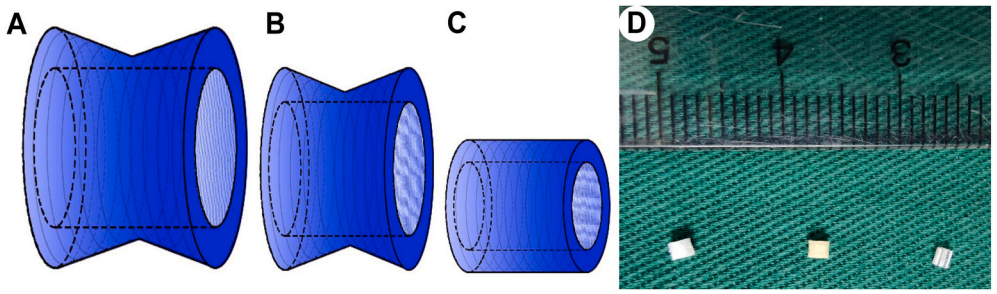

Fig. 4. Cuffs used for rat lung transplantation. All three cuffs were about 1.5 mm long. A: The cuff for the left main bronchus was made with a 14-G catheter. B: The cuff for the left pulmonary vein was made with a 16-G catheter. C: The cuff for the left pulmonary artery was made with an 18-G catheter. D: The three cuffs described above from left to right.

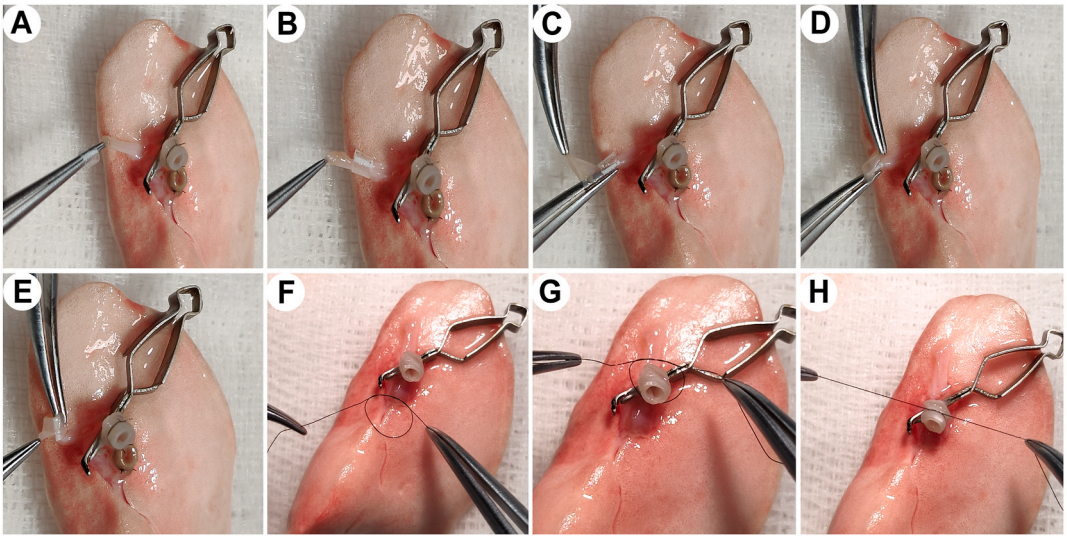

Fig. 5. Installation of the cuffs on the donor's left lung. A–E: The pulmonary artery passed through and was everted over the cuff. F–H: The cuff of the left main bronchus was fixed with a circumferential ligature of an 8–0 nylon suture.

2.6. Retrieval and preservation of the donor lung

After performing a midline laparotomy, we made a cross-shaped incision. Heparin was administered via the exposed abdominal vena cava at a dose of 1000 IU/kg. Five minutes later, we extended the laparotomy to the jaw. Subsequently, we severed the abdominal vena cava and aortaventralis, sheared the diaphragm along the chest wall, and rapidly opened the chest along the border between the rib cartilage and the rib bone on both sides. We excised the left and right auricles. Inserting the perfusion needle into the right ventricle until reaching the main pulmonary artery (Fig. 2A and B), we utilized our self-made perfusion device (Fig. 2*C*) to perfuse approximately 20 mL of 4 °C heparinized LPD solution (containing heparin 20 IU/mL) into the donor lung for no more than 5 min, under a pressure of 20 cm H_2O. Observing the color change of the lung from red to white, we sealed the gap between the main bronchus and the endotracheal intubation tube by applying pressure with fingers on the front neck of the rat. This step prevented air leakage and ensured full lung expansion. Subsequently, we clamped the main bronchus with a pair of toothed vascular forceps at maximum lung expansion and ligated it with a suture. Finally, we removed the inflated lung-heart block and immersed it in the 4 °C LPD solution for preservation (Video 1).

Supplementary data related to this article can be found online at https://doi.org/10.1016/j.heliyon.2024.e30728

2.7. Dissection of the donor's left pulmonary hilum

Thirty minutes before the transplantation anastomosis, we transferred the heart-lung block to an ice board from the LPD solution. We covered the left and right lobes with two pieces of LPD solution-soaked gauze and separated them as much as possible to expose the left pulmonary hilum, encompassing the left pulmonary artery, left main bronchus, and left pulmonary vein. The pulmonary vein appeared translucent and pale-yellow, distinct from the white, translucent left lower pulmonary ligament below and the white left main bronchus above. After excising the left lower pulmonary ligament, we bluntly dissected the left pulmonary vein (LPV) from the

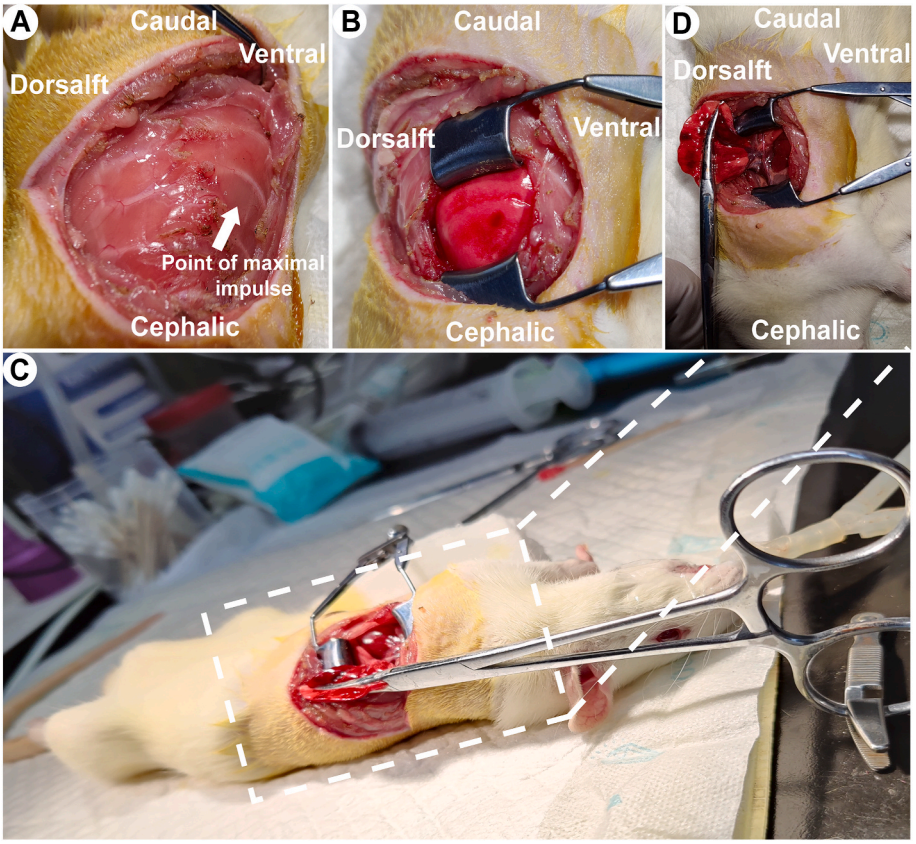

Fig. 6. Thoracotomy of the recipient rat. A–C: The rat was placed in the right decubitus position, and a third interspace thoracotomy was performed (where the heartbeat was the strongest). The incision was then dilated with an eyelid spreader. D: The left lung was pulled out of the chest and fixed with a mosquito clamp.

left main bronchus (LMB) at their boundary using micro-forceps (Fig. 3A and B). Subsequently, we severed the left pulmonary vein at the bifurcation of the left and right pulmonary veins (Fig. 3*C*). Employing micro-forceps with 0.3 mm tips, we proceeded to dissect the pulmonary hilum, install the cuffs, and perform tube anastomosis (involving the left pulmonary artery, vein, and left main bronchus). We then lifted and excised the left superior vena cava (LSVC), which traversed over the left pulmonary artery (LPA) and tightly adhered to the main pulmonary vein (Fig. 3D), thereby exposing the left pulmonary artery underneath (Fig. 3E). Subsequently, we dissociated and severed the left pulmonary artery at the bifurcation of the left and right pulmonary artery (Fig. 3F). Finally, we dissected and severed the left main trachea (MT) at the tracheal bifurcation (Video 2).

Supplementary data related to this article can be found online at https://doi.org/10.1016/j.heliyon.2024.e30728

2.8. Installation of the cuffs on the donor's left lung

We fashioned the cuffs from venous catheters of various sizes (Fig. 4), and all the cuffs' length was about 1.5 mm (Fig. 4D). To prevent slippage during subsequent procedures, we roughened the cuffs' surfaces using a surgical blade. Specifically, for the venous and tracheal cuffs, we shaped the cuffs' walls into a waist-shape using a surgical blade (Fig. 4A and B), and the artery cuff didn't need to be shaped (Fig. 4C). Subsequently, we extracted the left pulmonary artery, vein, and left main bronchus from an 18 G, 16 G, and 14 G cuff respectively (Fig. 5A and B). Only micro-forceps with tips smaller than 0.15 mm could navigate across the cuffs. Holding one side of the tube that had passed through the cuff with micro-forceps in the left hand, the operator utilized the right hand to grasp another micro-curved forceps and insert one of its tips into the tube lumen. Upon locating the tube lumen, we grasped both the tube wall and the cuff wall together with the forceps (Fig. 5C). Subsequently, the operator used the forceps in the left hand to secure the other side of the tube wall and folded it over the cuff (Fig. 5D). Then, the right hand held another forceps to fold the remaining side of the tube wall over the cuff (Fig. 5E). Finally, we affixed the tube's wall onto the cuff using an 8-0 suture loop (Fig. 5F, G, and H) (Video 3).

Supplementary data related to this article can be found online at https://doi.org/10.1016/j.heliyon.2024.e30728

2.9. Thoracotomy of the recipient

We positioned the anesthetized recipient rat in the right lateral position on the surgical board and intubated it. With an incision

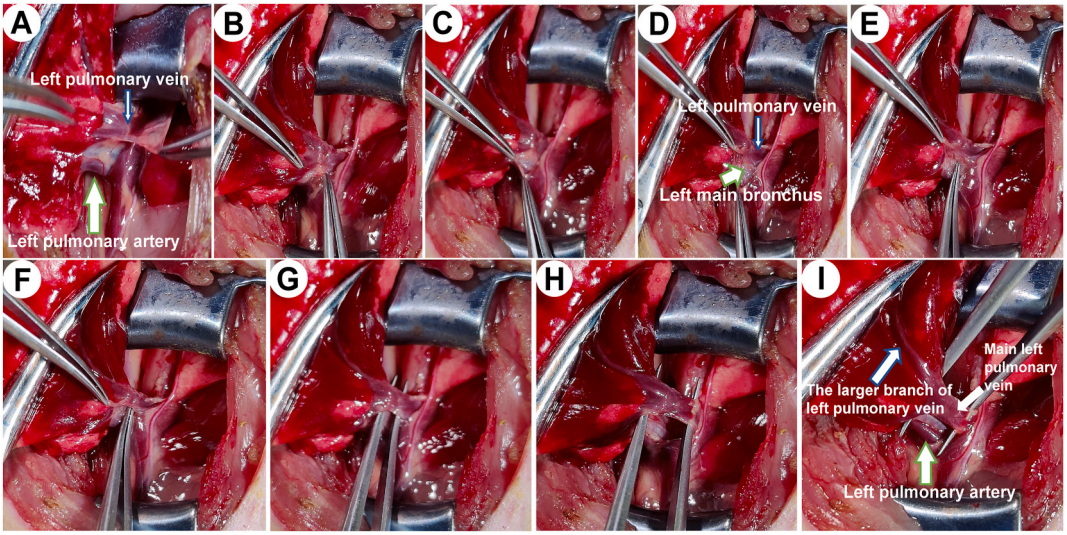

Fig. 7. Left pulmonary vein of the recipient was dissected. A–D: The pleural tissue around the left hilum was torn off. E–H: Insertion of the micro-forcep tips into the gap between the left main bronchus and the left pulmonary vein to separate the left pulmonary vein.

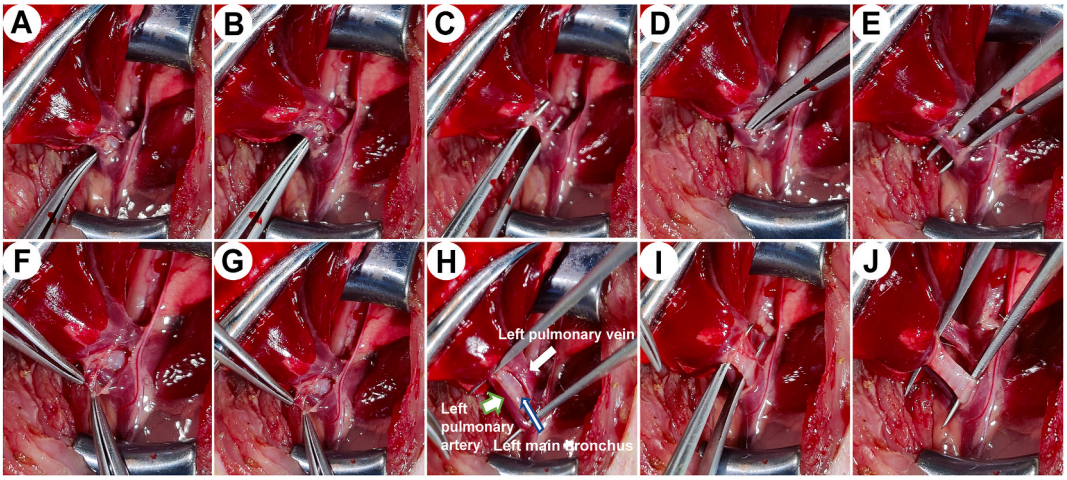

Fig. 8. Left pulmonary artery and the left main bronchus of the recipient were dissected. A–C: Insertion of the micro-forcep tips into the gap between the left pulmonary artery and the left main bronchus from the bottom up to separate the left pulmonary artery. D–E: Micro-forcep tips were inserted into the gap between the left pulmonary artery and the left main bronchus from the top down to separate the left pulmonary artery. F–G: The pleural tissue around the left pulmonary artery was torn off. H: Well-separated left pulmonary artery. I–J: The left main bronchus was lifted to be dissected.

along the upper edge of the fourth left rib in the third rib interspace—typically where the heartbeat was strongest—the chest was opened (Fig. 6A). This incision was made as close to the back as possible to prevent heart protrusion during surgery and ensure a clear surgical field. Using a blepharostat, we supported the chest wall incision (Fig. 6B). Subsequently, we adjusted the rat's position to a slightly left-elevated supine position (Fig. 6C) and used two cotton swabs to extract and fully extend the left lung, exposing the thickest and longest branch of the left pulmonary vein situated at the lower edge of the left lung. To stabilize it in place, we clamped the outer edge of the left lung with a mosquito hemostat (Fig. 6C and D) (Video 4).

Supplementary data related to this article can be found online at https://doi.org/10.1016/j.heliyon.2024.e30728

2.10. Dissection of the left pulmonary hilum of the recipient

Initially, we excised the ligamentous and pleural tissue surrounding the left pulmonary vein to expose the left pulmonary artery, left main bronchus, and left pulmonary vein (Fig. 7A–D). The operator positioned the tips of micro-bent forceps at the junction of the left pulmonary vein and the left main bronchus, then gently separated them (Fig. 7E–I).

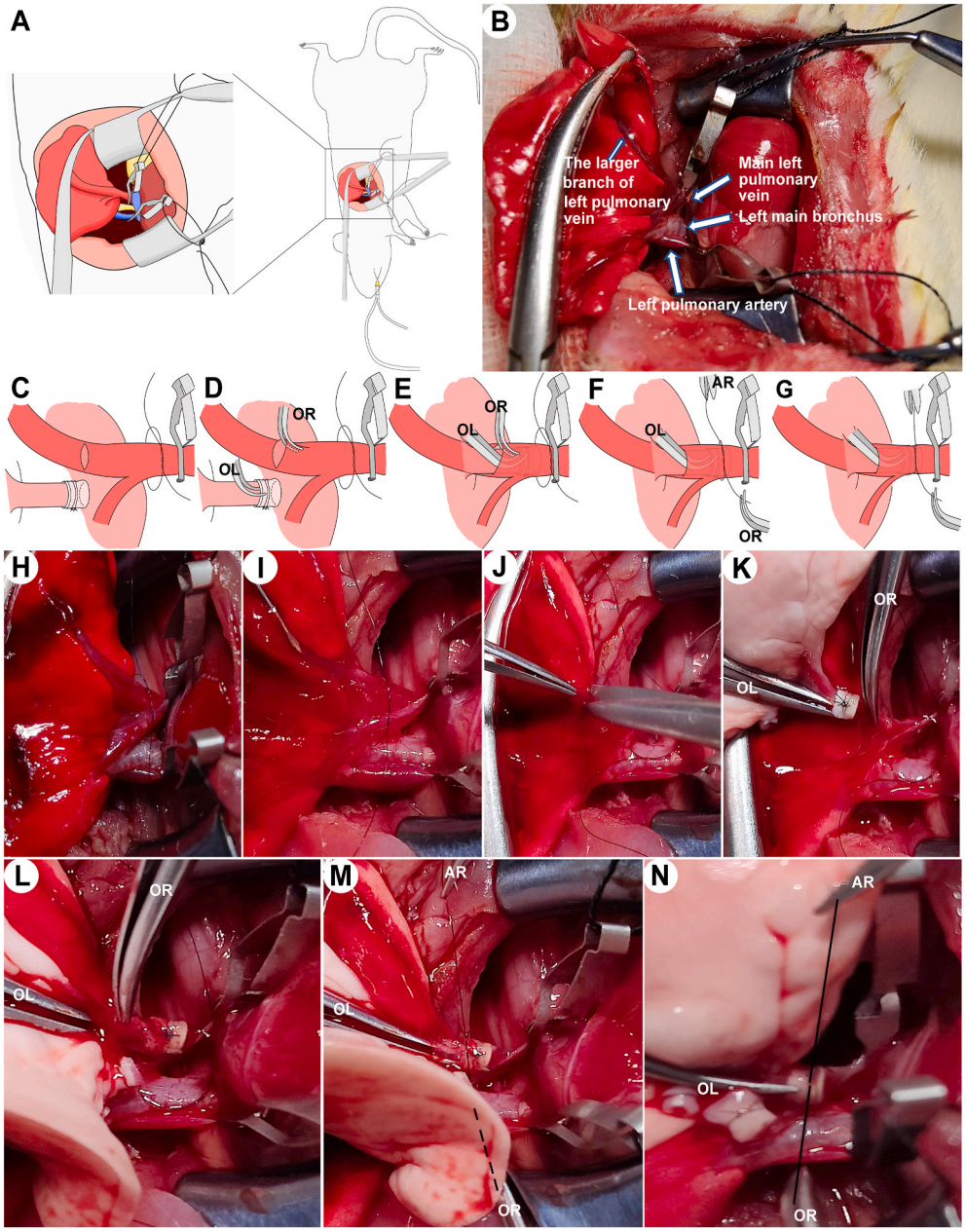

Fig. 9. Anastomosis of left pulmonary vein. A: Schematic illustration of the position of the recipient during anastomosis. The red left pulmonary vein and the blue left pulmonary artery were both clipped with microvascular clips. The yellow one was the left main bronchus. B: Photo of the anastomosis position. C–G: Animation of the sequence of venous anastomosis. H–N: Photos of the sequence of venous anastomosis. H: Unsecured surgical knot was indwelled before anastomosis. I: Heparin was injected into the branch of the left pulmonary vein before left pulmonary vein anastomosis. C and J: An incision was made on the giant branch of the left pulmonary vein. D and K: The operator lifted the upper wall of the left pulmonary vein on the proximal side of the incision with the forceps in the right hand (OR). E and L: The cuff was held and inserted into the incision with the left hand (OL). F and M: The forceps in the operator's right hand (OR) held one end of the suture, and the other end was held by the assistant's right hand (AR) to fasten the knot. J and N: The operator cooperated with the assistant to fasten the knot (the thin suture was indicated with a black auxiliary line). OR: the operator's right hand; OL: the operator's left hand; AR: the assistant operator's hand.

Subsequently, we inserted the tips of the micro-bent forceps beneath the pulmonary artery and pushed them upward near the boundary between the left pulmonary artery and the left main bronchus to bluntly separate the left pulmonary artery (Fig. 8A–C). Following this, the forceps were introduced into the artery-bronchus boundary from above the pulmonary artery to further separate the left pulmonary artery (Fig. 8D and E), ultimately detaching the envelope of the left pulmonary artery entirely (Fig. 8F–H). Finally, we dissociated the left main bronchus (Fig. 8I and J). To prevent obstruction of the surgical field, we clamped the left pulmonary artery

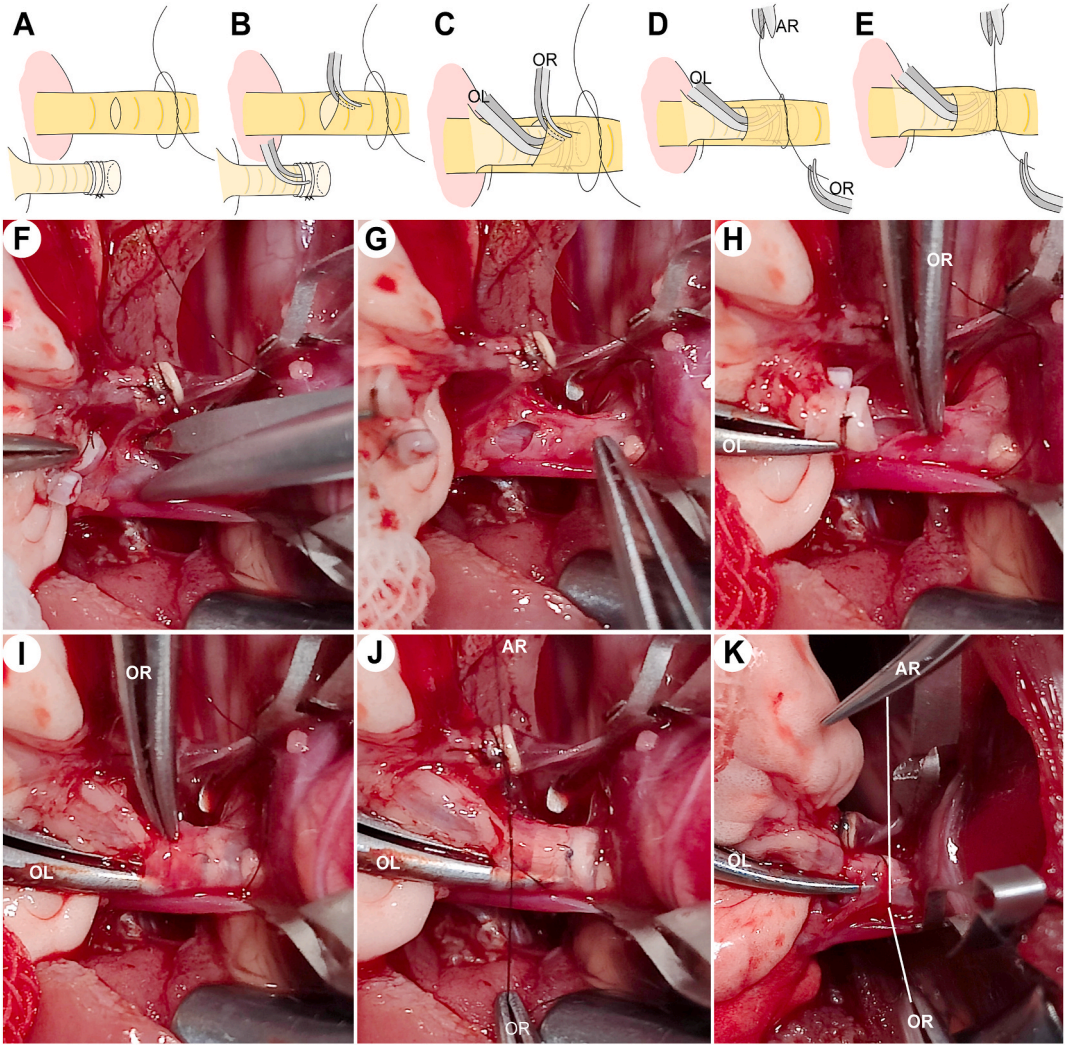

Fig. 10. Anastomosis of the left main bronchus. A–E: Animation of the bronchus anastomosis. F–K: Sequential photos of the bronchus anastomosis. A and F–G: An incision was made on the distal end of the trunk of the left main bronchus. B and H: The operator lifted the upper wall of the left main bronchus on the proximal side of the incision. C and I: The operator held the cuff and then inserted it into the incision. D and J: The forceps in the operator's right hand held one end of the suture, and the other end was held by the assistant's right hand. E and K: The knot was fastened (the thin suture is indicated with a white auxiliary line). OR: the operator's right hand; OL: the operator's left hand; AR: the assistant operator's hand.

and vein with microvascular hemostatic clips and secured the clips with surgical sutures to the blepharostat on both sides (Fig. 9A and B) (Video 4).

2.11. Anastomosis

Initially, we proceeded with the anastomosis of the left pulmonary vein (Fig. 9) (Video 5). Before venous anastomosis, it was crucial to secure an untightened surgical knot around the left pulmonary vein using an 8-0 surgical suture (nylon thread) (Fig. 9H), which was also essential for subsequent bronchial or arterial anastomosis. Subsequently, a small amount of sodium heparin solution was injected into the distal end of the thickest branch of the left pulmonary vein (Fig. 9I). While many researchers typically flushed the recipient's vascular bed after making the incision to prevent thrombosis, our experience showed that heparin injection effectively prevented vascular occlusion due to thrombosis. Then, an incision was cut on the distal end of the thickest branch of the left pulmonary vein (Fig. 9C and J). Care was taken to avoid excessive cutting of blood vessels, which could lead to complete disconnection, complicating the identification of the anastomotic stoma.

Supplementary data related to this article can be found online at https://doi.org/10.1016/j.heliyon.2024.e30728

Using a pair of micro-bent forceps held by the right hand, the operator elevated the proximal vessel wall of the incision to fully enlarge it into a hole (Fig. 9D and K). Simultaneously, another micro-bent forceps held by the left hand firmly grasped the cuff installed

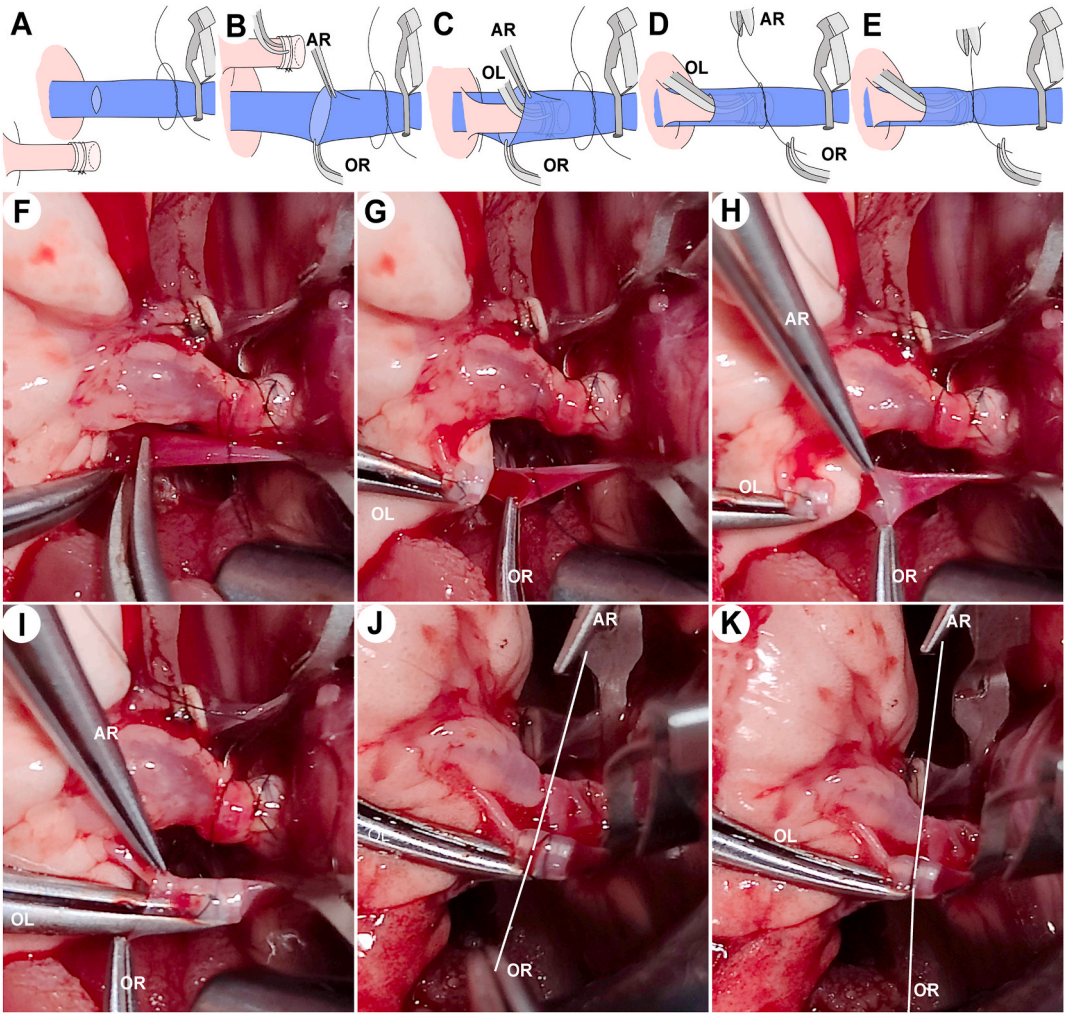

Fig. 11. Anastomosis of the left pulmonary artery. A–E: Animation of the artery anastomosis. F–K: Sequential photos of the artery anastomosis. A and F–G: An incision was made on the distal end of the left pulmonary artery. B and H: The assistant lifted the upper wall of the left pulmonary artery on the proximal side of the incision, and the operator pulled the lateral wall of the vessel to form an opening for inserting the cuff. C and I: The operator held the cuff and inserted it into the incision. D and J: The forceps in the operator's right hand held one end of the suture, and the other was held by the assistant's right hand. E and K: The operator cooperated with the assistant to fasten the knot (the thin suture is indicated with a white auxiliary line). OR: the operator's right hand; OL: the operator's left hand; AR: the assistant operator's hand.

on the donor's pulmonary vein, and the cuff was inserted into the incision until reaching the main trunk of the left pulmonary vein (Fig. 9E and L). It's worth noting that the pleura on the left pulmonary vein is firmly adhered to it, making it challenging to separate, and there is a risk of inserting the cuff into the space between the pleura and the left pulmonary vein wall, leading to a false anastomosis and subsequent pulmonary vein blockage after the operation. Once successfully inserted, one hand held the cuff in place (cuffs often slipped out of the incision without assistance, highlighting the necessity of an assistant), while the other hand used a needle holder to pull one end of the reserved knot, with the assistance of another person holding the other end of the reserved knot, ensuring fixation of the recipient's left pulmonary vein wall onto the cuff (Fig. 9F–G and M-N).

The anastomosis method for the left main bronchus was similar to that for the pulmonary vein, with the exception of heparinization (Fig. 10A–E and F-K) (Video 6). Prior to the anastomosis, we did not clamp the left main bronchus [19]. As such, the bronchus' cuff should be inserted into the incision quickly once the incision is made (less than 3s after the incision) to avoid the collapse of the right lung.

In addressing the left pulmonary artery (Fig. 11) (Video 7), once the knot was secured and heparinized, a small incision was made at the distal end of the left pulmonary artery (Fig. 11A and F). Due to the delicate nature of) the left pulmonary artery, expanding the incision into a hole required coordinated effort between the operator and the assistant: the operator pulled one side of the incision with their right hand (Fig. 11G), while the assistant lifted the proximal vessel wall of the incision to fully enlarge it (Fig. 11B and H). Meanwhile, the operator used their left hand to insert the cuff into the incision of the left pulmonary artery (Fig. 11C and I). Finally, both the operator and the assistant tightened the reserved knot to complete the anastomosis (Fig. 11D–E and J–K).

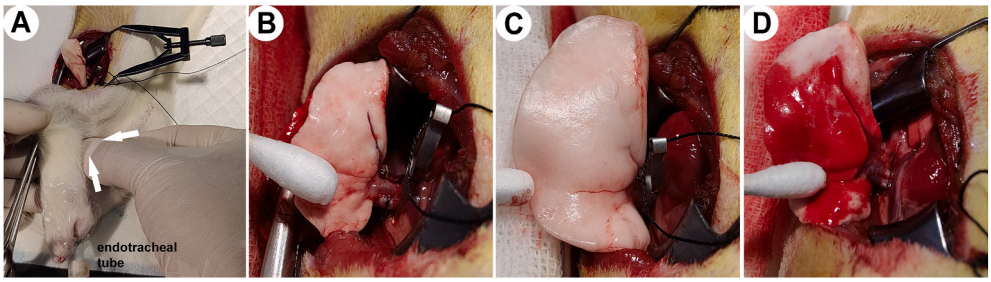

Fig. 12. Reperfusion initiating after anastomosis. A: The lacuna between the main trachea and the endotracheal tube was pressed to inflate the lungs sufficiently (white arrow indicates the press direction). B: Transplanted left lung before inflation. C: Transplanted left lung inflated fully. D: Transplanted left lung reperfusion for 3 s.

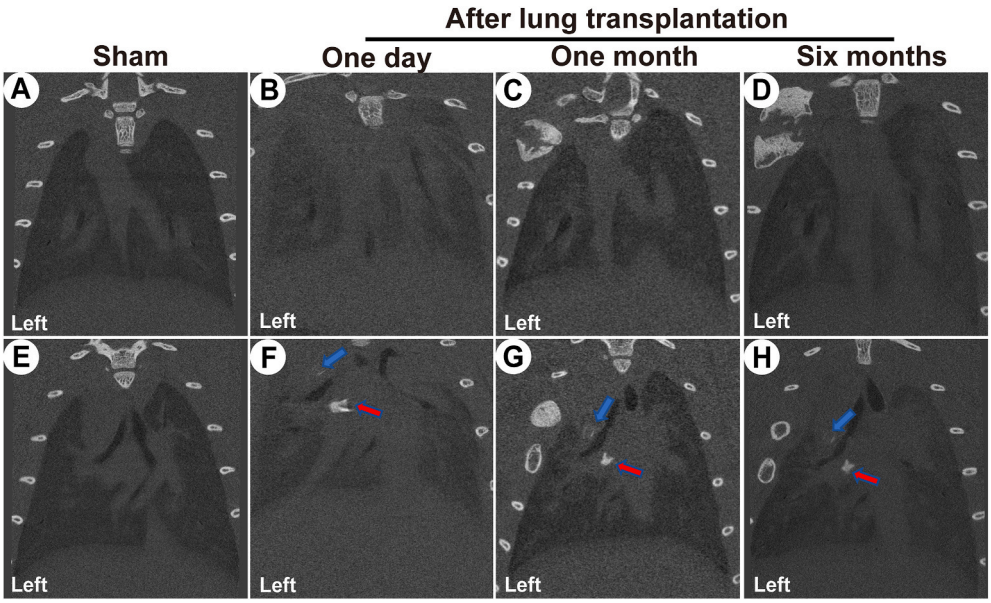

Fig. 13. CT (Computed Tomography) images of the transplanted lungs one day, one month, and six months after rat orthotopic left lung transplantation. A–D: CT layers showing the lungs with the maximum sectional area. E–H: CT showing the cuffs. B and F: Imaging examination showing diffuse exudation on both sides with pleural effusion one day after lung transplantation. The blue arrows indicate the cuffs of the left pulmonary artery and the red arrows indicate the cuffs of the left pulmonary vein. The cuff of the left main bronchus does not show up on the CT due to its material.

Supplementary data related to this article can be found online at https://doi.org/10.1016/j.heliyon.2024.e30728

2.12. Thoracotomy closure and post-anesthesia care

We completely removed the left lung stump of the recipient to ensure unrestricted blood flow and airflow. Initially, we removed the microvascular hemostatic clip from the left pulmonary vein, enabling immediate observation of blood flow, confirming the patency of the left pulmonary vein post-transplantation. Subsequently, pressure was applied to the anterior neck of the rat to close the gap between the main bronchus and the endotracheal intubation tube (Fig. 12A). We then fully inflated the transplanted left lung (Fig. 12B and C). Upon removal of the microsurgical hemostatic clip from the left pulmonary artery, the transplanted lung rapidly transitioned from a white to red hue (Fig. 12D). Following complete inflation of the left lung, we sutured the chest wall, gradually reducing the concentration of isoflurane. Administration of isoflurane ceased upon completion of suturing. Tracheal extubation was performed once the rat exhibited normal airway reflexes. Post-extubation, the rat was placed on an electric blanket for recovery. Upon full consciousness, the rat was transferred to a clean feeding box with ample food and water. Penicillin (80 IU/kg/24 h, administered via intramuscular injection) was administered continuously for seven days to prevent infection. Notably, Meloxicam (4 mg/kg/24 h, administered via subcutaneous injection) was provided continuously for seven days post-tracheal extubation for analgesia purposes.

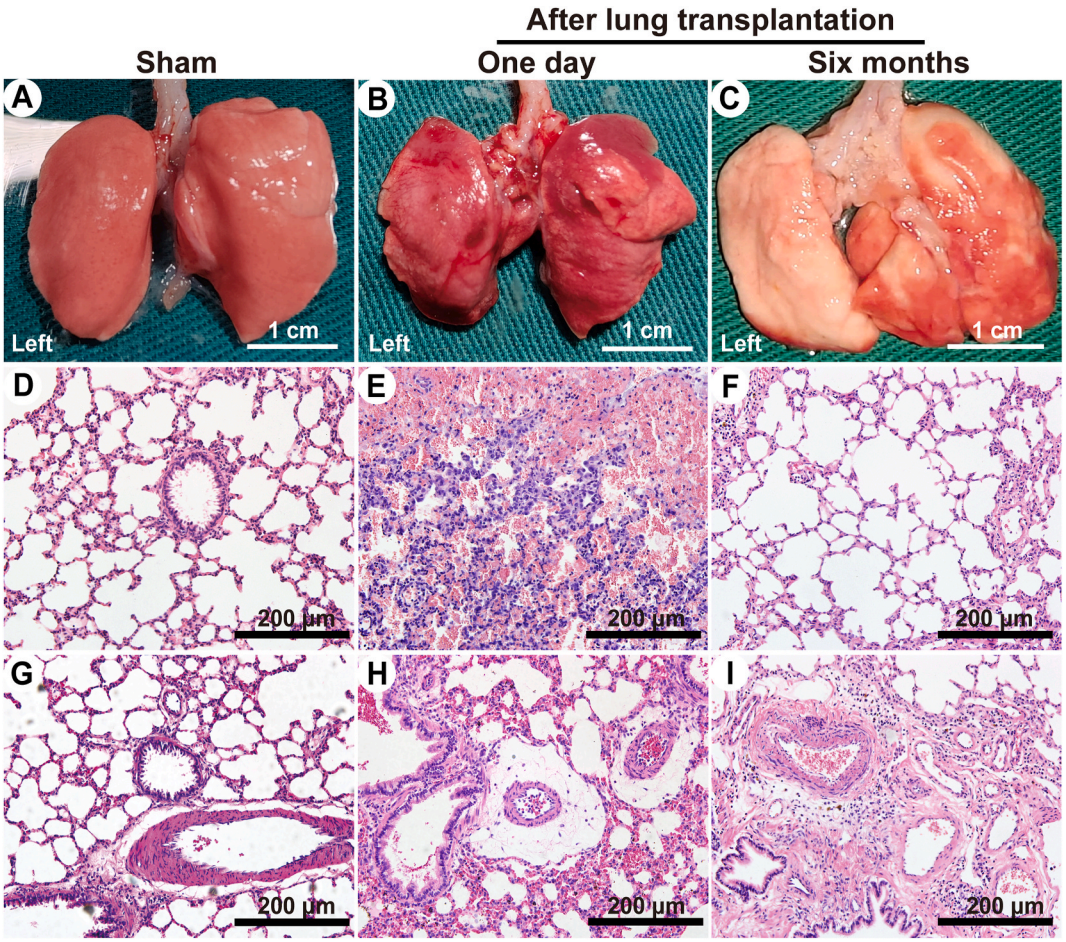

Fig. 14. Gross changes and Hematoxylin-Eosin (HE) staining of the rat lungs transplanted for one day and 6 months. A, B and C: Gross changes of the lungs. D, E and F: Alveolar field. G, H and I: Bronchovascular bundle field.

2.13. Micro CT analysis

Following anesthesia administration (30 mg/kg pentobarbital sodium, via intraperitoneal injection), we subjected the rats to micro-CT scanning (U-CT-XUHR, MILabs, Houten, The Netherlands). The lungs underwent reconstruction using the MILabs-Rec interface and were analyzed using IMALYTICS Preclinical 2.1 software (Gremse-IT GmbH, Germany).

2.14. Hematoxylin and eosin staining, Masson's trichrome staining

Subsequently, we sampled and fixed the transplanted left lungs of the rats in 10 % formalin for 24 h, followed by embedding in paraffin. The lungs were then sliced, and sections (4 μm thickness) were prepared for hematoxylin-eosin (HE) and Masson's trichrome staining. Morphological changes in the lungs were examined under a microscope (Olympus BX51, Japan) and photographed.

3. Results

In this investigation, we conducted sixty-four cases of rat orthotopic left lung transplantation, with one failure due to laceration of the recipient's left pulmonary vein. Among these cases, sixty-one were utilized for collecting statistical data, encompassing operation-related time and the survival rate at postoperative 4 h. Based on our experience during the initial learning phase, the 7-day mortality rate was nearly 0 % if recipient rats could recover and move freely within 2 h post-operation.

The time required for donor lung acquisition averaged (19 ± 4) minutes, while (11 ± 1) minutes were spent on donor lung hilum anatomy and cuff installation. Recipient thoracotomy and left lung hilar anatomy consumed (24 ± 8) minutes, with an additional (31 ± 6) minutes allotted for anastomosis. The survival rate at postoperative 4 h reached 96.7 %.

Regular postoperative computed tomography (CT) scans were conducted on the remaining three lung-transplanted rats (Fig. 13), two of which were euthanized one day and six months post-operation, respectively, for histopathological examination. One day after

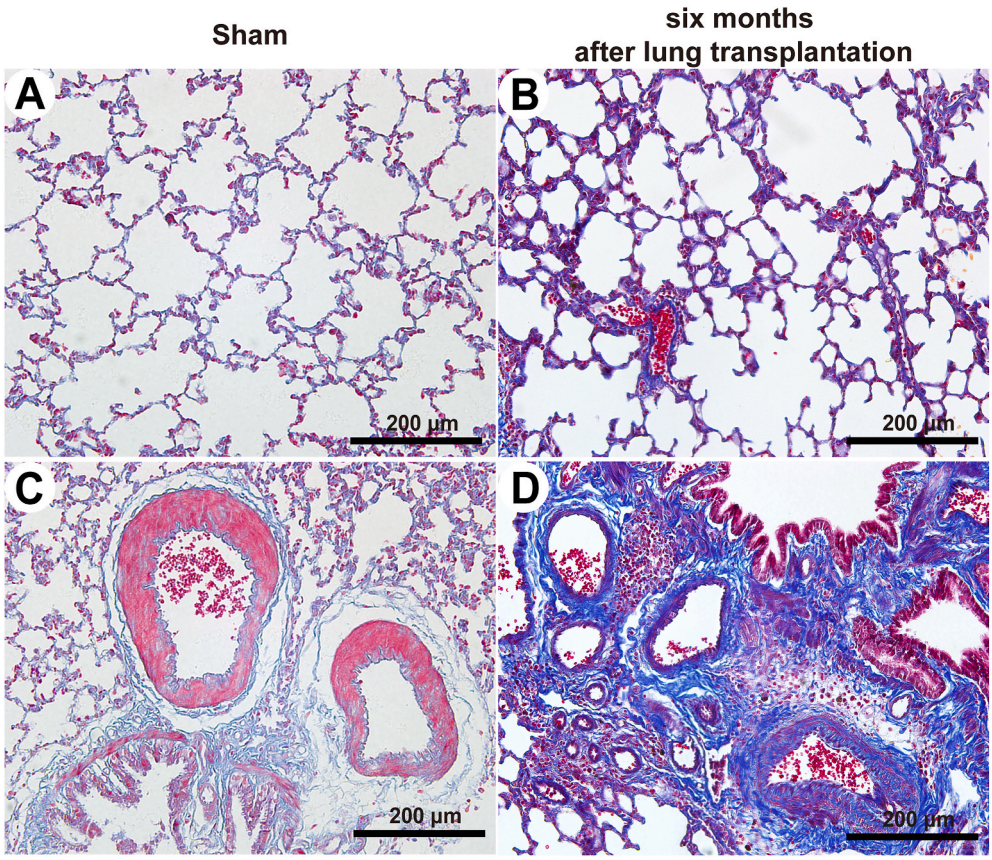

Fig. 15. Masson's staining of the rat lungs transplanted for 6 months. A and B: Alveolar field. C and D: Bronchovascular bundle field.

lung transplantation, both CT images (Fig. 13B and F) and gross appearance (Fig. 14B) revealed diffuse inflammation in both lungs of the rat in comparison with the sham control (Fig. 13A and E; Fig. 14A). The inflammation in the right lung might be attributed to ventilator-related injuries and exudate from the transplanted left lung. At one month (Fig. 13C and G) and six months (Fig. 13D and H) post-transplantation, CT images indicated sufficient inflation of the transplanted left lung, with no evident inflammation in either lung. Additionally, we observed inflation and contraction of the lung transplanted for six months (Fig. 14C) in accordance with ventilation rhythm under endotracheal intubation conditions prior to euthanasia.

We conducted HE staining (Fig. 14) and Masson staining (Fig. 15) on rat lung samples obtained one day and six months post-lung transplantation, respectively. HE staining revealed pronounced acute inflammation in the lung transplanted for one day (Fig. 14E and H) in comparison with the sham control (Fig. 14D and G), characterized by: 1) Accumulation of exudate and erythrocytes within the alveolar cavity; 2) Thickening of the alveolar wall indicative of alveolar epithelial cell swelling; 3) Evident perivascular area edema; and 4) Notable infiltration of inflammatory cells. After six months, HE staining (Fig. 14F and I) and Masson staining (Fig. 15) illustrated chronic pathological alterations in comparison with the sham control (Fig. 14D and G; Fig. 15A and C), including: 1) Hyperplasia of pulmonary interstitial fibers and reduction in alveolar cells (Fig. 15B); 2) Extensive microvascular hyperplasia (Fig. 15D); and 3) Marked leukocyte infiltration surrounding vessels and the trachea (Fig. 14I). These findings suggest that the rat lung transplantation model described herein serves as a valuable tool for investigating both acute and chronic respiratory complications post-lung transplantation.

4. Discussion

In our investigation, we employed a modified three-cuff technique to streamline and enhance the rat lung transplantation procedure. The rat orthotopic left lung transplantation model, characterized by its cost-effectiveness, accurately mimics clinical lung transplantation and is well-suited for studying both acute pathological changes and chronic diseases post-transplantation. Additionally, the size advantage of rats facilitates the utilization of auxiliary devices in experiments, such as ex vivo lung perfusion (EVLP) [20] and extracorporeal membrane oxygenation (ECMO) [21].

Although the cuff technique for rat lung transplantation was initially proposed by Takatoshi Mizuta in 1989 [15], the orthotopic left lung transplantation model in rats has not been widely adopted due to the procedure's complexity and intricacy. Currently, the left lung hilar clamping model [22] and the heterotopic tracheal transplantation model remain the primary models for studying lung

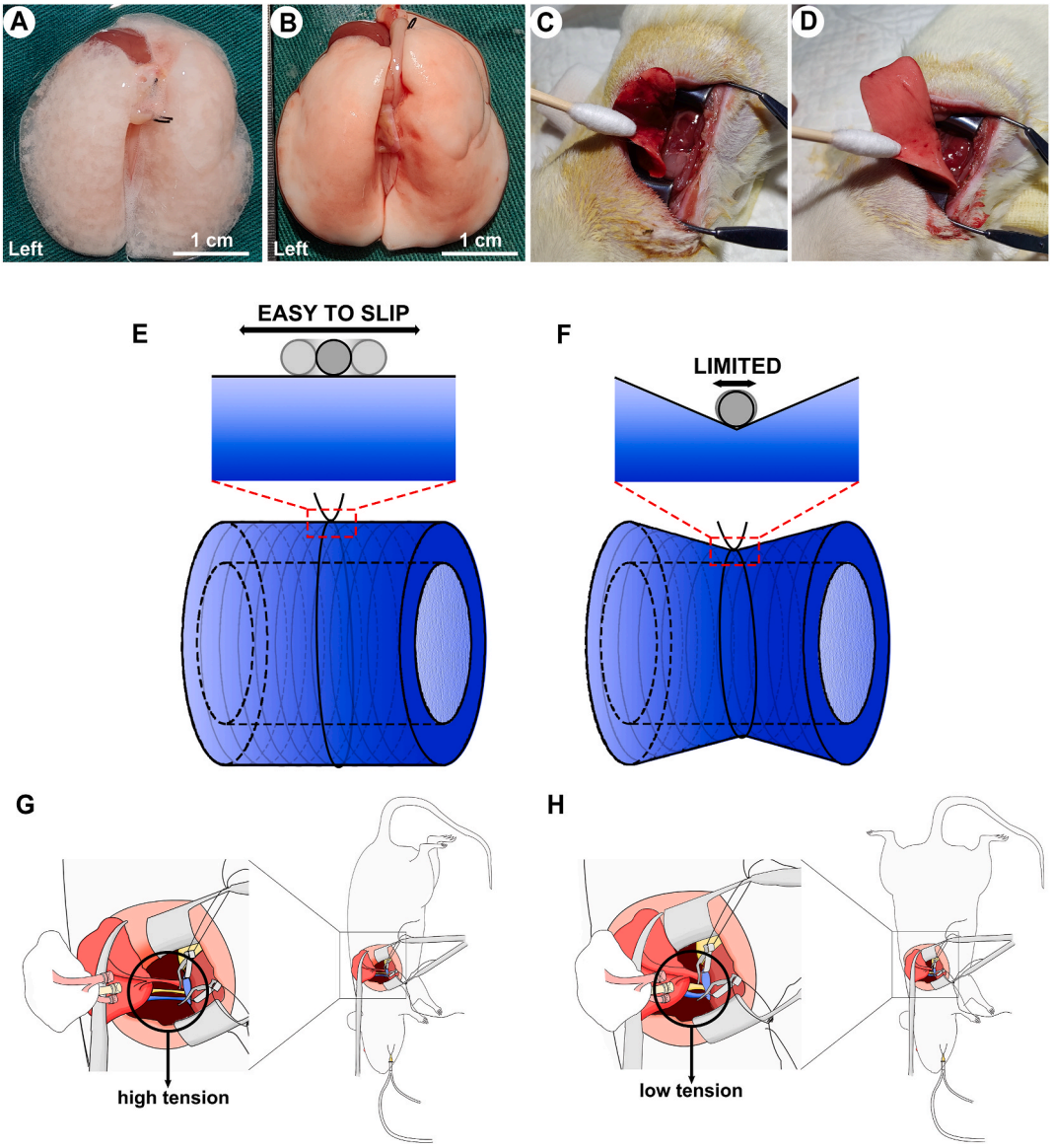

Fig. 16. Advantages of the modified rat lung transplantation model. A: Edema donor lung caused by manual injection of perfusion fluid. B: Donor lung perfused with the self-made perfusion device. C: Postoperative transplanted lung atelectasis caused by uninflated preservation. D: A well-expanded transplanted lung with new donor lung preservation method. E: Traditional anastomosis cuff. F: Modified anastomosis cuff in the study. G: The left lung hilar had high tension with the right lateral position of the recipient rat. H: The left lung hilar had lower tension with the slightly left elevated supine position of the recipient rat.

transplantation. However, an indispensable lung transplantation model is crucial for simulating the cold ischemia-reperfusion process, which directly impacts primary graft dysfunction (PGD) [23] and is a significant contributor to graft failure [24].

Furthermore, some studies have utilized rodent lung transplantation models to investigate the molecular mechanisms of metastasis of various cancers to the lung [25]. Additionally, with the capability to establish rodent lung transplantation models, researchers can develop other relevant animal models, such as the left main bronchus ligation model [26].

While the mouse lung transplantation model may be suitable for certain experiments [7,27–30], including many that we and other researchers have conducted, it has been observed that the successful implementation of rat lung transplantation modeling significantly reduces the learning curve for mouse lung transplantation [30].

Therefore, an easily learnable rat lung transplantation model holds significant importance for basic research in lung transplantation and related lung diseases. In this investigation, we enhanced the procedures of the rat orthotopic left lung transplantation model to make it more accessible for researchers.

Elimination of microscope surgery: We introduced the first comprehensive method for left lung orthotopic transplantation in rats

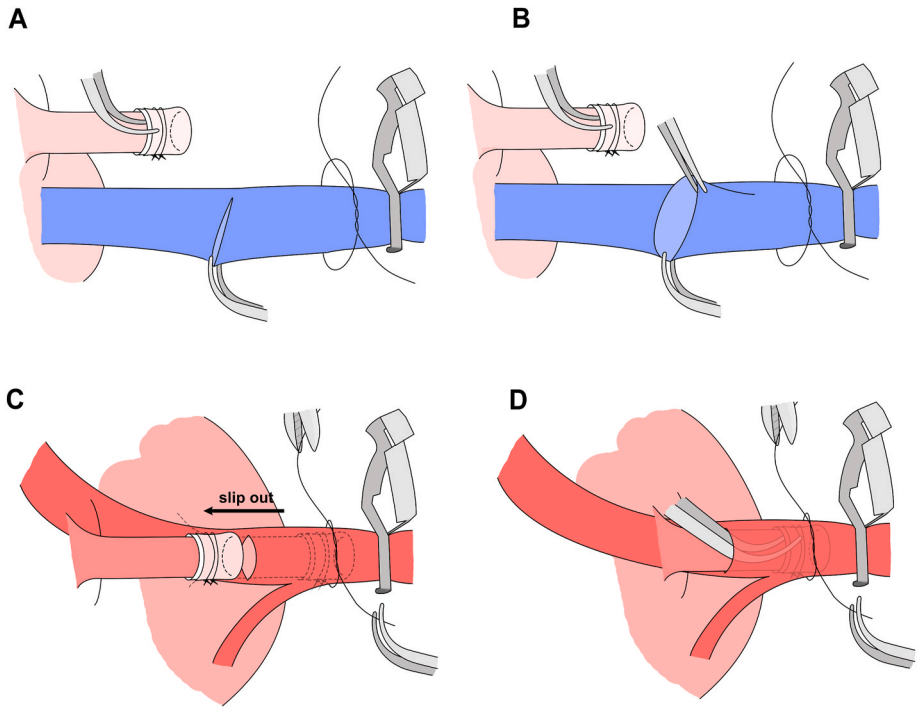

Fig. 17. Advantages of the modified anastomosis technique. A: The collapsed incision makes it difficult for the cuff to be inserted into. B: With an assistant lifting the incision wall, a large enough hole allows the cuff to be inserted smoothly. C: The cuff always slips out from the incision when the operator fastens the knot. D: The operator grips the cuff to keep it inside the incision, and fastens the knot with an assistant, avoiding cuff slippage.

without the need for a microscope. We also provided the most detailed anatomical diagrams of the left lung hilar region. Surgical microscopy typically demands extensive training and poses significant challenges in maintaining aseptic conditions and coordinating assistance. However, we demonstrated that rat left lung orthotopic transplantation can be effectively performed without a surgical microscope, yielding a high success rate.

Introduction of a new intubation method: While previous studies have suggested orotracheal intubation in rats under direct vision [31], and video laryngoscopes have been employed in subsequent studies [32], our novel oblique position endotracheal intubation method significantly reduces the complexity of the procedure. Moreover, this method can be adapted for endotracheal intubation in mice.

Implementation of a new perfusion instrument: Traditional manual injection methods often result in vascular rupture and lung edema (Fig. 16A). To address this issue, we developed a self-made perfusion device capable of maintaining constant perfusion pressure, thereby preventing vascular damage and lung edema (Fig. 16B). Additionally, our perfusion method using the self-made device can facilitate the removal of blood cells from rat or mouse lungs before tissue fixation for pathological examinations [33], thereby minimizing variations in pathology due to sampling methods.

Introduction of a new donor lung preservation method: Studies aiming to mitigate primary graft dysfunction (PGD) often involve preserving donor lungs for more than 12 h [34]. However, traditional methods of cold preservation typically lags always behind lung dissection, leading to gas leakage and preservation fluid permeation in lung tissue. This results in difficulty re-expanding transplanted lungs post-surgery (Fig. 16C). In our study, we initiated hours of cold perfusion prior to lung dissection, maintaining donor lung inflation as much as possible during the preservation and surgery. This approach significantly reduces the likelihood period, which greatly reduced the probability of atelectasis following the surgery (Fig. 16D).

New anastomosis cuffs: We developed new anastomosis cuffs to address a common issue during anastomosis, where the suture loop often slips off from traditional cuffs (Fig. 16E). Our solution involves inventing a waist-shaped cuff with a thin middle and thick ends, preventing the suture loop from slipping (Fig. 16F). This innovation effectively prevents anastomosis failure due to suture loop slippage and can also be utilized in other rodent vascular or tube anastomosis procedures employing the cuff technique [35].

New surgical position: We implemented a new surgical position to overcome challenges associated with accessing the lung hilar during transplantation. The lung hilar is deeply situated within the chest, making it is more challenging to transplant a rodent lung compared to a liver or kidney. While most researchers perform rat or mouse lung hilar anastomosis in a right lateral position, this approach often results in high lung hilar tension and lacerations of vessels or bronchi during dissection and anastomosis (Fig. 16G). In contrast, we adopted a slightly left elevated supine position, significantly reducing lung hilar tension during anastomosis (Fig. 16H).

New anastomosis technique: We introduced a new anastomosis technique to address two of the most challenging and critical aspects of both rat and mouse lung transplantation procedures. These include effectively inserting the cuffs into their corresponding

Table 1
Comparison of our protocol to other methods for preparation of lung transplantation models in rat or mice.

Surgical Steps	Basic Requirements	Improvements Made in Other Studies	Methods and Improvements in Our Study	Advantages of Our Protocol
1 Perfusion of the donor lung	Perfuse with a certain pressure. The perfusion device description is not clear.	1 Insert the intravenous indwelling needle into the pulmonary artery to perfuse and then retrogradely perfuse through the pulmonary vein [32,37]. 2 Inject directly into the pulmonary artery with a syringe [29]. 3 Using an unknown gravity perfusion device for perfusion [38].	A simple self-made perfusion device is used for perfusion. It is made from a 50 mL syringe and a disposable intravenous infusion needle. The perfusion pressure is maintained at about 20 cm H_2O.	The perfusion pressure is constant, and the device is simple and convenient to acquire with high operability.
2 Preservation and infusion solution	4 °C LPD solution.	1 A hydrogen-rich solution [39]. 2 ET-Kyoto solution [40]. 3 Cold LPD solution with sodium bicarbonate [41]. 4 4 °C heparinized LPD solution [42].	4 °C heparinized LPD solution (heparin concentration is 20 IU/mL).	High concentration of heparin sodium can effectively prevent microthrombus formation. Heparin can also reduce lung injury by inhibiting cell pyroptosis [43].
3 Preservation method of the Inflated donor lung	The donor lung should be full-inflated.	1 The donor lung is semi-inflated [37,42]. 2 The donor lung is semi-inflated with 50 % O_2[38].	With the left and right lungs of the donor fully inflated, the main trachea is tied with a suture. Do not disconnect the right lung and heart and immerse the entire heart-lung block in 4 °C heparinized LPD solution. The left lung is separated before transplantation.	The heart-lung block inflated fully as a whole unit could prevent atelectasis after transplantation and guarantee better allograft function post-transplantation [44].
4 Description of the vessels' cutting position of the donor	There is no accurate description.		The donor's left pulmonary artery and vein should be completely dissociated to their proximal end, and we cut off them there.	Enough length of the vessels eases the cuff-installation and further anastomosis.
5 Cuff style	Cuffs with tail.	1 Cuffs with round tail [45]. 2 The cuffs' surface is notched to increase friction [29,46]. 3 Cuffs without tail [42,47].	Pare the out wall of the cuff to shape it with a narrow waist and notch some scratches on the surface.	Reshaping the cuff could increase friction and prevent suture slippage during the installation of the cuffs and anastomosis. Waist-shaped cuffs makes griping of the cuff's body firmer than its tail. It avoids the exposed tail squeezing the trachea and vessels.
6 Posture of the recipient in surgery	Right lateral position.	Right-half supine position with anterior hilum anastomosis [48].	Slightly left elevated supine position.	The supine position significantly reduces the tension at the recipient's left hilum, reducing the risk of vascular tear.
7 Method for blocking the recipient's left pulmonary hilum	Clamp the hilum altogether with a pair of microvascular forceps.	1 Ligate the left pulmonary artery and vein with a 22G venous catheter, respectively [32]. 2 Clamp the left pulmonary artery/vein/bronchus with microvascular hemostatic clips [37,41,46,47]. 3 Ligate the three structures in the hilum with surgical sutures individually [42]. 4 Clamp the left pulmonary artery and vein with microvascular hemostatic clips and ligate the bronchus with a surgical suture [9]. 5 Ligate the vessels with surgical sutures and clamp	Clamp the left pulmonary artery and vein with microvascular hemostatic clips. Fix the clips with sutures to the blepharostat on both sides. Do not block the recipient's bronchus.	The microvascular hemostatic clip is easy to operate. Fixing the clips could eliminate the impact their shaking caused by cardiac and arterial pulsation on the surgical field. Once the bronchus was anastomosed successfully, the transplanted lung would inflate with the ventilation rhythm and sufficient inflation could prevent atelectasis after transplantation. The unclamped bronchus could also serve as a reminder of whether there is air leakage or blockage.

(*continued on next page*)

Table 1 (*continued*)

Surgical Steps	Basic Requirements	Improvements Made in Other Studies	Methods and Improvements in Our Study	Advantages of Our Protocol
		the bronchus with a microclip [29,49]. 6 Clamp the left pulmonary artery and vein with microclips, and don't clamp the bronchus [30,38]. 7 Ligate the vein with a surgical suture and clamp the bronchus and artery with microclips [50].		
8 Management of the recipient's left lung stump during anastomosis	The recipient's left lung stump is fixed with an instrument. A small incision is made on the left pulmonary artery/vein/bronchus.	Cut off the recipient's left lung stump with the left pulmonary artery/vein/bronchus. Fix the cuffs of the donor's left lung with an instrument when anastomosis [29,41].	The left lung stump is clamped with mosquito vascular forceps to immobilize and expose the recipient's left lung hilum.	The remaining left lung stump could provide a solid platform for vascular and tracheal anastomosis without extra instruments.
9 Anastomotic incision	There are no mainstream yet personalized methods, including: 1 The anastomotic incisions of the recipient's three tubes are all "—" shape incision on their trunk [42,47]. 2 The anastomotic incision of the recipient's left pulmonary vein is a triangle incision on its trunk [13]. 3 The left pulmonary artery's anastomotic incision is a "T" -shaped and the vein and bronchus are "V"-shaped [45]. 4 Cut a small incision on the inferior branch of left pulmonary vein rather than the trunk [49]. 5 The left pulmonary vein's anastomotic incision is arc-shaped on its trunk [28].		"—" type incisions are made at the thickest branch of the recipient's left pulmonary vein, the distal end of the left pulmonary artery and the bronchus, respectively. Only about 1/3 of the circumferential diameter of the three tubes is cut off when making incisions.	The "—" incision is simple and avoids tearing or completely severing of the three tubes caused by complicated incisions. The uncut part of the tubes can provide a fulcrum for anastomosis, avoiding extra pulling with other instruments.
10 Anastomosis	The left pulmonary artery, vein and left main bronchus are all anastomosed with the cuff technique.	1 Use the cuff technique to anastomose the left pulmonary artery and vein with bronchial suturing [9,15]. 2 All these three tubes (left pulmonary artery, vein, and left main bronchus) are anastomosed with the cuff technique, but the cuff for the bronchus is installed in the lumen like a stent [32]. 3 The tubes of both donor and recipient are all installed with cuffs, and then anastomose them with the aorta of the donor [46]. 4 The tubes are anastomosed with suturing technique [50].	All are anastomosed with the standard cuff technique.	The requirement for microsurgical skills of the operator is not as high. Anastomosis is convenient and fast. Avoids scar contracture and occlusion of the lumen after suturing [29].
11 Administration of heparin during anastomosis	Heparin is applied locally to the anastomotic incision.		Heparin should be injected into the recipient's left pulmonary vein from its distal end before the anastomosis incision is made. It should also be added dropwise to the artery's anastomosis incision immediately after the incision.	There is still a period before reperfusion after the anastomosis of the left pulmonary vein. During this period, a thrombus can easily form in the anastomosed left pulmonary vein. The injection of heparin in the left pulmonary vein in advance can prevent thrombus formation.
12 Maneuver of preliminary anastomosis	There is no accurate description.		As for the anastomosis of the left pulmonary vein and left main bronchus, the operator holds the forceps in the right hand to lift the proximal up wall of the anastomosis incision to form a clear hole while using the left hand's forceps to insert the cuff into the hole. As for the	Our anastomosis maneuver is simplified and patterned.

(*continued on next page*)

Table 1 (*continued*)

Surgical Steps	Basic Requirements	Improvements Made in Other Studies	Methods and Improvements in Our Study	Advantages of Our Protocol
			anastomosis of the left pulmonary artery, the operator holds the forceps in the right hand to pull the side wall of the anastomosis incision, and the assistant uses the forceps to lift the proximal up wall to form a clear hole.	
13 Maneuver of fixing the cuff after preliminary anastomosis	After inserting a cuff into the tube of the recipient, the cuff would be temporarily fixed depending on the elastic contraction force of the tube. It would then be secured with a suture loop.	Insert the cuff into the anastomotic incision, and use forceps to clamp the cuff, the tube's wall of the recipient, and one side of the reserved suture loop tightly while another pair of forceps pull another side of the loop to fasten it [47].	After inserting the cuff into the anastomotic incision, the operator holds the cuff in the lumen and cooperate with the assistant to fasten the suture loop with another hand.	Our maneuver prevents the cuffs from pulling away from the anastomotic incision, and knotting with the help of an assistant reduces the operator's surgical ability requirements.
14 Method of lung recruitment after anastomosis	There is no accurate description.	1 Increase PEEP to 5 cm H_2O before the reperfusion [37]. 2 Temporary hyperbaric expansion and high PEEP after the reperfusion [50].	Before the reperfusion, gently press the space between the trachea and the endotracheal intubation tube closed with fingers to inflate the transplanted left lung fully.	Most rat endotracheal intubation tubes do not have a balloon, resulting in insufficient gas filling into the transplanted lung. Our maneuver could inflate the lungs conveniently, reducing the pulmonary vascular resistance of the transplanted lung and ensuring even reperfusion [13].
15 Opening order of the three hilum tubes after anastomosis	Because the hilum is clamped by a pair of microvascular forceps, all three tubes open together after removing the vascular forceps.	1 First, anastomose the left pulmonary artery and bronchus, and then open the artery and bronchus. After the transplanted lung recruitment and its vein outflow of blood, clamp the artery and bronchus again to anastomose the vein, and open the left pulmonary vein, bronchus, and artery in that order [37]. 2 First, open the left main bronchus to inflate the transplanted lung, then open the vein and artery successively [30,38,47]. 3 Open the left main bronchus, pulmonary vein, and artery in sequence [9]. 4 Open the left pulmonary vein, main bronchus, and pulmonary artery in sequence [50].	First, open the vein to observe the retrograde flow and then inflate the transplanted lung sufficiently. Finally, open the artery to start reperfusion.	Releasing the vein first allows observing of its blood backflow, an essential safeguard for venous anastomosis quality. We can then deal with venous anastomosis accidents on time [13].

LPD: low-potassium dextran; PEEP: positive end-expiratory pressure.

anastomosis incisions and minimizing tensile force from the donor lung to prevent the cuffs from dislodging before fixation. The inability to smoothly insert cuffs into incisions due to incision collapse often leads to vascular laceration, a primary cause of operation failure with traditional anastomosis methods (Fig. 17A). In our approach, we propose the assistance of a second person to lift the incision wall, creating a sufficiently large hole for smooth cuff insertion (Fig. 17B).

Furthermore, the cuffs frequently slip out from incisions when operators tighten the knot (Fig. 17C). To mitigate this issue, our method involves, the operator gripping the cuff to keep it inside the incision while an assistant tightens the knot (Fig. 17D), effectively preventing cuff slippage. While it is commonly believed that completing an animal model with a single person is ideal, the complexity of organ transplantation presents numerous challenges that a single operator may struggle to overcome easily.

Our anastomosis methods involve simple assistance from a second person, significantly reducing the precision required for surgical operation, the time spent on repeated attempts, and the likelihood of operating errors. This approach ensures smoother and more efficient procedures without requiring extensive surgical training for the assistant.

Furthermore, particularly in the realm of chronic disease models post-lung transplantation research, we observed that rats undergoing our lung transplantation model could survive for at least six months post-operation with favorable lung conditions. This

extended survival period allows for the simulation of pathological changes occurring over a longer duration following lung transplantation. Consequently, we assert that our modifications to the rat orthotopic left lung transplantation model render it suitable for studying chronic complications post-lung transplantation.

However, our study presents certain some limitations. Firstly: we lacked a sufficient number of rat lung transplant samples to verify the long-term (beyond 6 months) survival of the graft. Secondly, the absence of transgenic mutants in rat models limits our ability to explore molecular mechanisms [36].

Overall the disparities between our protocol and those of existing rat or mouse lung transplantation models (details provided in Table 1) highlight noticeable advantages of our approach. These include reduced preparation time and a more feasible and concise operation, rendering it easier for adoption.

5. Conclusions

We present a modified rat orthotopic left lung transplantation model characterized by reduced modeling time and enhanced operability. This model is capable of simulating both acute and long-term chronic processes following lung transplantation.

Ethics statement

Approval for this study was granted by the Experimental Animal Welfare Ethics Committee of Zhejiang University (ZJU20220159). All procedures were conducted in accordance with the animal welfare and ethics guidelines of Zhejiang University.

Funding

This research received support from the Zhejiang Provincial Natural Science Foundation of China under grants LZ20H010001, LY16H010004.

Data availability statement

Data will be provided upon reasonable request.

CRediT authorship contribution statement

Jinsheng Li: Writing – review & editing, Writing – original draft, Methodology, Formal analysis, Data curation. **Yifan Yu:** Writing – review & editing, Methodology, Formal analysis, Data curation. **Lingjun Dong:** Writing – review & editing, Formal analysis, Data curation. **Zhiling Lou:** Writing – review & editing, Formal analysis, Data curation. **Qiuyu Fang:** Writing – review & editing, Methodology, Formal analysis, Data curation. **Fuxiang Liang:** Writing – review & editing, Formal analysis, Data curation. **Yangfan Li:** Writing – review & editing, Formal analysis, Data curation. **Ming Wu:** Writing – review & editing, Writing – original draft, Supervision, Resources, Project administration, Methodology, Funding acquisition, Conceptualization.

Declaration of competing interest

The authors declare that they have no known competing financial interests or personal relationships that could have appeared to influence the work reported in this paper.

References

[1] R.M. Kotloff, G. Thabut, Lung transplantation, Am. J. Respir. Crit. Care Med. 184 (2) (2011) 159–171, https://doi.org/10.1164/rccm.201101-0134CI.
[2] C.S. Harris, H.J. Lee, I.S. Alderete, et al., The cost of lung transplantation in the United States: how high is too high? JTCVS Open (2024) https://doi.org/10.1016/j.xjon.2024.01.010. Published online January 21.
[3] M. Capuzzimati, O. Hough, M. Liu, Cell death and ischemia-reperfusion injury in lung transplantation, J. Heart Lung Transplant. 41 (8) (2022) 1003–1013, https://doi.org/10.1016/j.healun.2022.05.013.
[4] J.D. Christie, R.M. Kotloff, V.N. Ahya, et al., The effect of primary graft dysfunction on survival after lung transplantation, Am. J. Respir. Crit. Care Med. 171 (11) (2005) 1312–1316, https://doi.org/10.1164/rccm.200409-1243OC.
[5] J.B. Orens, E.R. Garrity, General overview of lung transplantation and review of organ allocation, Proc. Am. Thorac. Soc. 6 (1) (2009) 13–19, https://doi.org/10.1513/pats.200807-072GO.
[6] H. Huang, H.J. Yan, X.Y. Zheng, et al., Right lung transplantation with a left-to-right inverted anastomosis in a rat model, JTCVS Open 10 (2022) 429–439, https://doi.org/10.1016/j.xjon.2022.01.020.
[7] A.D. Giannou, B. Ohm, D.E. Zazara, et al., Protocol for orthotopic single-lung transplantation in mice as a tool for lung metastasis studies, STAR Protoc 4 (4) (2023) 102701, https://doi.org/10.1016/j.xpro.2023.102701.
[8] J.F. Gielis, W. Jungraithmayr, G.A. Boulet, et al., A murine model of lung ischemia and reperfusion injury: tricks of the trade, J. Surg. Res. 194 (2) (2015) 659–666, https://doi.org/10.1016/j.jss.2014.12.008.
[9] B. Kubisa, R.A. Schmid, T. Grodzki, Model of single left rat lung transplantation. Relation between surgical experience and outcomes, Rocz Akad Med Bialymst 48 (2003) 70–73.
[10] L. Ma, B. Fei, Comprehensive review of surgical microscopes: technology development and medical applications, J. Biomed. Opt. 26 (1) (2021) 010901, https://doi.org/10.1117/1.JBO.26.1.010901.
[11] L.S. Ming, K.C. Yew, A.B. Chong, Common errors in the use of the operating microscope, Aust. J. Opthalmol. 6 (1) (1978) 16–19, https://doi.org/10.1111/j.1442-9071.1978.tb00248.x.

[12] B.M.D. Russi, C.A.M. Carvalho, Anatomic and embryological aspects of the cardiovascular system of Albino Wistar rats, J. Morphol. Sci. 36 (4) (2019) 317–320, https://doi.org/10.1055/s-0039-1697008.
[13] T.K. Rajab, Anastomotic techniques for rat lung transplantation, World J. Transplant. 8 (2) (2018) 38–43, https://doi.org/10.5500/wjt.v8.i2.38.
[14] P.J. Asimacopoulos, F.A. Molokhia, C.A. Pegg, J.C. Norman, Lung transplantation in the rat, Transplant. Proc. 3 (1) (1971) 583–585.
[15] T. Mizuta, A. Kawaguchi, K. Nakahara, Y. Kawashima, Simplified rat lung transplantation using a cuff technique, J. Thorac. Cardiovasc. Surg. 97 (4) (1989) 578–581.
[16] W. Li, H.M. Shepherd, A.S. Krupnick, A.E. Gelman, K.J. Lavine, D. Kreisel, Mouse heterotopic cervical cardiac transplantation utilizing vascular cuffs, J. Vis. Exp. 184 (2022), https://doi.org/10.3791/64089.
[17] W. Wu, J. Yuan, F. Liu, et al., Research progress on anatomy reconstruction of rat orthotopic liver transplantation, Transplant. Rev. 38 (2) (2024) 100841, https://doi.org/10.1016/j.trre.2024.100841.
[18] Z.D. Jin, L.N. Xue, L.S. Peng, Orthotopic kidney transplantation in the rat with the use of a sleeve arterial anastomosis method and a modified stenting technique for renal veins, Transplant. Proc. 49 (8) (2017) 1942–1946, https://doi.org/10.1016/j.transproceed.2017.04.022.
[19] W. Jungraithmayr, W. Weder, The technique of orthotopic mouse lung transplantation as a movie-improved learning by visualization, Am. J. Transplant. 12 (6) (2012) 1624–1626, https://doi.org/10.1111/j.1600-6143.2011.03980.x.
[20] A. Ohsumi, T. Kanou, A. Ali, et al., A method for translational rat ex vivo lung perfusion experimentation, Am. J. Physiol. Lung Cell Mol. Physiol. 319 (1) (2020) L61–L70, https://doi.org/10.1152/ajplung.00256.2019.
[21] J. Huang, R. Zhang, K. Zhai, et al., Venovenous extracorporeal membrane oxygenation promotes alveolar epithelial recovery by activating Hippo/YAP signaling after lung injury, J. Heart Lung Transplant. 41 (10) (2022) 1391–1400, https://doi.org/10.1016/j.healun.2022.06.005.
[22] E. Koletsis, A. Chatzimichalis, E. Apostolakis, et al., In situ cooling in a lung hilar clamping model of ischemia-reperfusion injury, Exp. Biol. Med. 231 (8) (2006) 1410–1420, https://doi.org/10.1177/153537020623100815.
[23] J. Zhao, J. Li, D. Wei, et al., Liproxstatin-1 alleviates lung transplantation-induced cold ischemia-reperfusion injury by inhibiting ferroptosis, Transplantation (2023), https://doi.org/10.1097/TP.0000000000004638. Published online May 19.
[24] W. Tian, Y. Liu, B. Zhang, et al., Infusion of mesenchymal stem cells protects lung transplants from cold ischemia-reperfusion injury in mice, Lung 193 (1) (2015) 85–95, https://doi.org/10.1007/s00408-014-9654-x.
[25] A.D. Giannou, J. Kempski, A.M. Shiri, et al., Tissue resident iNKT17 cells facilitate cancer cell extravasation in liver metastasis via interleukin-22, Immunity 56 (1) (2023) 125–142.e12, https://doi.org/10.1016/j.immuni.2022.12.014.
[26] K. Shiraishi, P.P. Shah, M.P. Morley, et al., Biophysical forces mediated by respiration maintain lung alveolar epithelial cell fate, Cell 186 (7) (2023) 1478–1492.e15, https://doi.org/10.1016/j.cell.2023.02.010.
[27] Z. Mei, M. Taheri, E.A. Jacobsen, et al., A simple cuff technique for murine left lung transplantation, J. Vis. Exp. 203 (2024), https://doi.org/10.3791/65979.
[28] M. Okazaki, A.S. Krupnick, C.G. Kornfeld, et al., A mouse model of orthotopic vascularized aerated lung transplantation, Am. J. Transplant. 7 (6) (2007) 1672–1679, https://doi.org/10.1111/j.1600-6143.2007.01819.x.
[29] A.S. Krupnick, X. Lin, W. Li, et al., Orthotopic mouse lung transplantation as experimental methodology to study transplant and tumor biology, Nat. Protoc. 4 (1) (2009) 86–93, https://doi.org/10.1038/nprot.2008.218.
[30] W.M. Jungraithmayr, S. Korom, S. Hillinger, W. Weder, A mouse model of orthotopic, single-lung transplantation, J. Thorac. Cardiovasc. Surg. 137 (2) (2009) 486–491, https://doi.org/10.1016/j.jtcvs.2008.10.007.
[31] A.L. Rivard, K.J. Simura, S. Mohammed, et al., Rat intubation and ventilation for surgical research, J. Invest. Surg. 19 (4) (2006) 267–274, https://doi.org/10.1080/08941930600778297.
[32] P. Gao, C. Li, Y. Ning, et al., Improvement of surgical techniques for orthotopic single lung transplantation in rats, Ann. Transl. Med. 10 (12) (2022) 673, https://doi.org/10.21037/atm-22-2018.
[33] M.L. Davenport, T.P. Sherrill, T.S. Blackwell, M.D. Edmonds, Perfusion and inflation of the mouse lung for tumor histology, J. Vis. Exp. 162 (2020), https://doi.org/10.3791/60605, 10.3791/60605.
[34] T. Kanou, A. Ohsumi, H. Kim, et al., Inhibition of regulated necrosis attenuates receptor-interacting protein kinase 1-mediated ischemia-reperfusion injury after lung transplantation, J. Heart Lung Transplant. 37 (10) (2018) 1261–1270, https://doi.org/10.1016/j.healun.2018.04.005.
[35] S. Cho, I.H. Song, Cuff technique for small-diameter vascular grafts in the systemic arterial circulation of the rat, Korean J Thorac Cardiovasc Surg 51 (6) (2018) 423–426, https://doi.org/10.5090/kjtcs.2018.51.6.423.
[36] J.H. Lin, Applications and limitations of genetically modified mouse models in drug discovery and development, Curr. Drug Metabol. 9 (5) (2008) 419–438, https://doi.org/10.2174/138920008784746355.
[37] N. Santana Rodríguez, P. Llontop Santisteban, A. López García, et al., Technical modifications of the orthotopic lung transplantation model in rats with brain-dead donors, Arch. Bronconeumol. 47 (10) (2011) 488–494, https://doi.org/10.1016/j.arbres.2011.05.003.
[38] T.K. Rajab, Techniques for lung transplantation in the rat, Exp. Lung Res. 45 (9–10) (2019) 267–274, https://doi.org/10.1080/01902148.2019.1675806.
[39] M. Saito, T.F. Chen-Yoshikawa, M. Takahashi, et al., Protective effects of a hydrogen-rich solution during cold ischemia in rat lung transplantation, J. Thorac. Cardiovasc. Surg. 159 (5) (2020) 2110–2118, https://doi.org/10.1016/j.jtcvs.2019.09.175.
[40] E. Miyamoto, H. Motoyama, M. Sato, et al., Association of local intrapulmonary production of antibodies specific to donor major histocompatibility complex class I with the progression of chronic rejection of lung allografts, Transplantation 101 (5) (2017) e156–e165, https://doi.org/10.1097/TP.0000000000001665.
[41] A. Habertheuer, A. Kocher, G. Laufer, et al., Innovative, simplified orthotopic lung transplantation in rats, J. Surg. Res. 185 (1) (2013) 419–425, https://doi.org/10.1016/j.jss.2013.05.006.
[42] H. Guo, J. Nie, K. Fan, et al., Improvements of surgical techniques in a rat model of an orthotopic single lung transplant, Eur. J. Med. Res. 18 (2013) 1, https://doi.org/10.1186/2047-783X-18-1.
[43] R. Yang, X. Zhang, A potential new pathway for heparin treatment of sepsis-induced lung injury: inhibition of pulmonary endothelial cell pyroptosis by blocking hMGB1-LPS-induced caspase-11 activation, Front. Cell. Infect. Microbiol. 12 (2022) 984835, https://doi.org/10.3389/fcimb.2022.984835.
[44] Y. Tanaka, N. Shigemura, K. Noda, et al., Optimal lung inflation techniques in a rat lung transplantation model: a revisit, Thorac. Cardiovasc. Surg. 62 (5) (2014) 427–433, https://doi.org/10.1055/s-0034-1373902.
[45] D. Tian, H. Shiiya, M. Sato, J. Nakajima, Rat lung transplantation model: modifications of the cuff technique, Ann. Transl. Med. 8 (6) (2020) 407, https://doi.org/10.21037/atm.2020.02.46.
[46] T. Goto, M. Kohno, M. Anraku, T. Ohtsuka, Y. Izumi, H. Nomori, Simplified rat lung transplantation using a new cuff technique, Ann. Thorac. Surg. 93 (6) (2012) 2078–2080, https://doi.org/10.1016/j.athoracsur.2012.01.096.
[47] W. Zhai, J. Ge, I. Inci, et al., Simplified rat lung transplantation by using a modified cuff technique, J. Invest. Surg. 21 (1) (2008) 33–37, https://doi.org/10.1080/08941930701834114.
[48] J. Zhao, D. Tian, X. Yang, M. Liu, J. Chen, Anterior hilum anastomosis versus posterior hilum anastomosis in a mouse lung transplantation model, JTCVS Tech 14 (2022) 159–165, https://doi.org/10.1016/j.xjtc.2022.04.019.
[49] T. Mizobuchi, Y. Sekine, K. Yasufuku, T. Fujisawa, D.S. Wilkes, Comparison of surgical procedures for vascular and airway anastomoses that utilize a modified non-suture external cuff technique for experimental lung transplantation in rats, J. Heart Lung Transplant. 23 (7) (2004) 889–893, https://doi.org/10.1016/j.healun.2003.06.009.
[50] Q chun Zhang, D jun Wang, N. Yin, et al., The orthotopic left lung transplantation in rats: a valuable experimental model without using cuff technique, Transpl. Int. 21 (11) (2008) 1090–1097, https://doi.org/10.1111/j.1432-2277.2008.00747.x.